

University of Wollongong

Research Online

Australian Institute for Innovative Materials -
Papers

Australian Institute for Innovative Materials

1-1-2014

90° magnetic coupling in a NiFe/FeMn/biased NiFe multilayer spin valve component investigated by polarized neutron reflectometry

S J. Callori

University of New South Wales

J Bertinshaw

University of New South Wales

David L. Cortie

University of Wollongong, dlc422@uowmail.edu.au

J W. Cai

Chinese Academy of Sciences

A P. Le Brun

ANSTO

See next page for additional authors

Follow this and additional works at: <https://ro.uow.edu.au/aiimpapers>



Part of the [Engineering Commons](#), and the [Physical Sciences and Mathematics Commons](#)

Research Online is the open access institutional repository for the University of Wollongong. For further information contact the UOW Library: research-pubs@uow.edu.au

90° magnetic coupling in a NiFe/FeMn/biased NiFe multilayer spin valve component investigated by polarized neutron reflectometry

Abstract

We have observed 90° magnetic coupling in a NiFe/FeMn/biased NiFe multilayer system using polarized neutron reflectometry. Magnetometry results show magnetic switching for both the biased and free NiFe layers, the latter of which reverses at low applied fields. As these measurements are only capable of providing information about the total magnetization within a sample, polarized neutron reflectometry was used to investigate the reversal behavior of the NiFe layers individually. Both the non-spin-flip and spin-flip neutron reflectometry signals were tracked around the free NiFe layer hysteresis loop and were used to detail the evolution of the magnetization during reversal. At low magnetic fields near the free NiFe coercive field, a large spin-flip signal was observed, indicating magnetization aligned perpendicular to both the applied field and pinned layer.

Keywords

femn, nife, reflectometry, coupling, neutron, magnetic, 90, polarized, investigated, component, valve, spin, multilayer, biased

Disciplines

Engineering | Physical Sciences and Mathematics

Publication Details

Callori, S. J., Bertinshaw, J., Cortie, D. L., Cai, J. W., Le Brun, A. P., Zhu, T. & Klose, F. (2014). 90° magnetic coupling in a NiFe/FeMn/biased NiFe multilayer spin valve component investigated by polarized neutron reflectometry. *Journal of Applied Physics*, 116 (3), 033909-1-033909-5.

Authors

S J. Callori, J Bertinshaw, David L. Cortie, J W. Cai, A P. Le Brun, T Zhu, and Frank Klose



90° magnetic coupling in a NiFe/FeMn/biased NiFe multilayer spin valve component investigated by polarized neutron reflectometry

S. J. Callori, J. Bertinshaw, D. L. Cortie, J. W. Cai, A. P. Le Brun, T. Zhu, and F. Klose

Citation: [Journal of Applied Physics](#) **116**, 033909 (2014); doi: 10.1063/1.4890355

View online: <http://dx.doi.org/10.1063/1.4890355>

View Table of Contents: <http://scitation.aip.org/content/aip/journal/jap/116/3?ver=pdfcov>

Published by the [AIP Publishing](#)

Articles you may be interested in

[Highly sensitive linear spin valve realized by tuning 90° coupling in a NiFe/thin IrMn/biased NiFe structure through nonmagnetic spacer insertion](#)

[J. Appl. Phys.](#) **109**, 094504 (2011); 10.1063/1.3585701

[Magnetization reversal mechanisms in Heusler alloy spin valves](#)

[J. Appl. Phys.](#) **109**, 07B110 (2011); 10.1063/1.3551592

[Influence of IrMn exchange bias layer on the magnetic properties of half-ring NiFe micron structures](#)

[J. Appl. Phys.](#) **101**, 09F511 (2007); 10.1063/1.2711175

[Interlayer segregation of Cu atoms in Ta/NiFe/Cu/NiFe/FeMn/Ta spin-valve multilayers and its influence on magnetic properties](#)

[J. Appl. Phys.](#) **91**, 3759 (2002); 10.1063/1.1450033

[Magnetic and thermal relaxation in \(NiFe/CoFe\)/PtMn and NiFe/NiMn bi-layers for spin valve heads](#)

[J. Appl. Phys.](#) **87**, 6424 (2000); 10.1063/1.372726

Advances in Live Single-Cell Thermal Imaging and Manipulation International Symposium, November 10-12, 2014

biophysics; soft condensed matter/soft mesoscopics; IR/terahertz spectroscopy
single-molecule optoelectronics/nanoplasmonics; photonics; living matter physics

Application deadline: August 24



OIST

OKINAWA INSTITUTE OF SCIENCE AND TECHNOLOGY GRADUATE UNIVERSITY
沖縄科学技術大学院大学



90° magnetic coupling in a NiFe/FeMn/biased NiFe multilayer spin valve component investigated by polarized neutron reflectometry

S. J. Callori,^{1,2,a)} J. Bertinshaw,^{1,2} D. L. Cortie,^{3,2} J. W. Cai,^{4,b)} A. P. Le Brun,² T. Zhu,⁴ and F. Klose^{2,5}

¹*School of Physics, The University of New South Wales, Sydney, New South Wales 2052, Australia*

²*Bragg Institute, Australian Nuclear Science and Technology Organization, Lucas Heights, New South Wales 2234, Australia*

³*The Institute for Superconducting and Electronic Materials, The University of Wollongong, Wollongong, New South Wales 2522, Australia*

⁴*Institute of Physics, Chinese Academy of Sciences, Beijing 100190, China*

⁵*Department of Physics and Materials Science, City University of Hong Kong, Hong Kong*

(Received 4 May 2014; accepted 4 July 2014; published online 17 July 2014)

We have observed 90° magnetic coupling in a NiFe/FeMn/biased NiFe multilayer system using polarized neutron reflectometry. Magnetometry results show magnetic switching for both the biased and free NiFe layers, the latter of which reverses at low applied fields. As these measurements are only capable of providing information about the total magnetization within a sample, polarized neutron reflectometry was used to investigate the reversal behavior of the NiFe layers individually. Both the non-spin-flip and spin-flip neutron reflectometry signals were tracked around the free NiFe layer hysteresis loop and were used to detail the evolution of the magnetization during reversal. At low magnetic fields near the free NiFe coercive field, a large spin-flip signal was observed, indicating magnetization aligned perpendicular to both the applied field and pinned layer. © 2014 AIP Publishing LLC. [<http://dx.doi.org/10.1063/1.4890355>]

I. INTRODUCTION

Since the advent of giant magnetoresistance based magnetic memory devices, spin valve (SV) structures have played an important role in technological applications of magnetic materials. SVs consist of a layered free ferromagnet (FM)/nonmagnetic material/biased FM/antiferromagnet (AFM) geometry, and it is desirable that these sensors have linear, non-hysteretic, and reversible resistive responses to external magnetic fields. In order to accomplish this, these systems must be designed so that the magnetization within the free FM layer is perpendicularly oriented to the magnetization within the biased FM layer.¹

Many avenues towards developing SVs with perpendicular in-plane magnetization configurations have relied on complex sensor designs,^{2–5} which can be disadvantageous for the optimization of these devices. A promising approach to simplify the construction of SVs while achieving perpendicular magnetizations is through exchange bias systems, via FM/AFM/FM trilayer structures^{6–8} or through similar trilayers with ferrimagnetic spacers.^{9,10} However, many AFM and ferrimagnets require complicated growth conditions for incorporation into SV devices. Liu *et al.* have recently put forth work on SVs constructed with NiFe FM layers separated by an AFM spacer layer of Ir₂₅Mn₇₅ (IrMn),¹ an additional layer of which is also used to pin the biased NiFe layer through exchange bias. The advantage of these SVs is that both NiFe and IrMn are commonly used materials in layered industrial magnetic devices, with IrMn inducing strong exchange bias and exhibiting good thermal stability.¹¹ In

principle, similar multilayer stacks with any other conventional AFM and FM materials can exhibit such a 90° coupling, and should also be directly applied to magnetic tunnel junctions for linear sensor applications and thus are technologically very important. Here, we aim to investigate the coupling between the free and biased NiFe layers in a multilayer system that forms a component of the SVs originally presented by Liu *et al.*¹ (See Fig. 1 in Ref. 1).

For the systems noted above, previous experiments have reported on the observation of perpendicular coupling between free and biased FM layers at zero field. The majority of these results, however, have relied on bulk magnetometry measurements. While magnetometry is a powerful technique, it is only capable of providing information about the total magnetization within a sample along the direction of the applied field. Polarized neutron reflectometry (PNR) is capable of resolving both the nuclear and magnetic structures of magnetic thin films and layers.^{12,13} PNR allows access to the in-plane magnetization vectors both along and perpendicular to the applied field as a function of layer depth. Using PNR enabled us to make a direct measurement of perpendicular coupling that unambiguously identifies the orientations of the free and biased FM layers and investigate the reversal mechanisms that enable this behavior.

II. EXPERIMENT

The NiFe/FeMn/pinned NiFe multilayer presented here was grown on water-cooled thermally oxidized Si substrate in a multisource sputtering chamber. A diagram of the layered structure is shown in Fig. 1. During growth, a field of roughly 30 mT was applied in the film plane to induce an easy axis in the ferromagnetic layers. The top NiFe layer

^{a)}Electronic mail: sara.callori@ansto.gov.au

^{b)}Electronic mail: jwcai@aphy.iphys.ac.cn

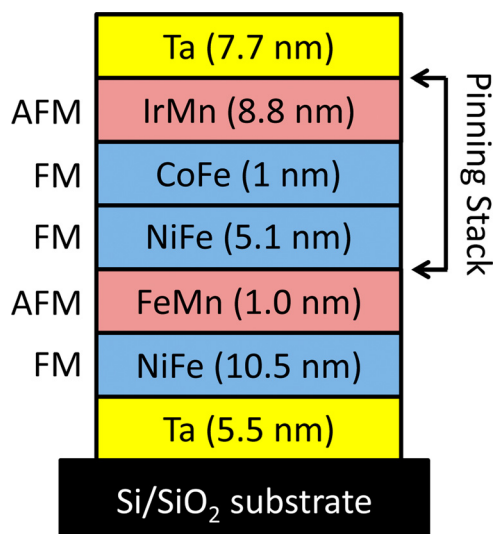


FIG. 1. Schematic of the NiFe/FeMn/biased NiFe multilayer structure. The numbers in parentheses are the thickness of each layer.

was pinned by a FM/AFM $\text{Co}_{50}\text{Fe}_{50}/\text{Ir}_{25}\text{Mn}_{75}$ (CoFe/IrMn) bilayer. Below the pinning stack, a free NiFe layer was separated from the stack by a thin spacer layer $\text{Fe}_{50}\text{Mn}_{50}$ (FeMn), another typical AFM. A Ta buffer layer was deposited prior to the NiFe stack and was used to promote [111] texture to avoid a three-dimensional growth mode of NiFe. An additional Ta layer capped the structure to prevent oxidation.

Magnetometry measurements were conducted using a vibrating sample magnetometer at room temperature and are shown in Fig. 2. M-H hysteresis measurements were used to

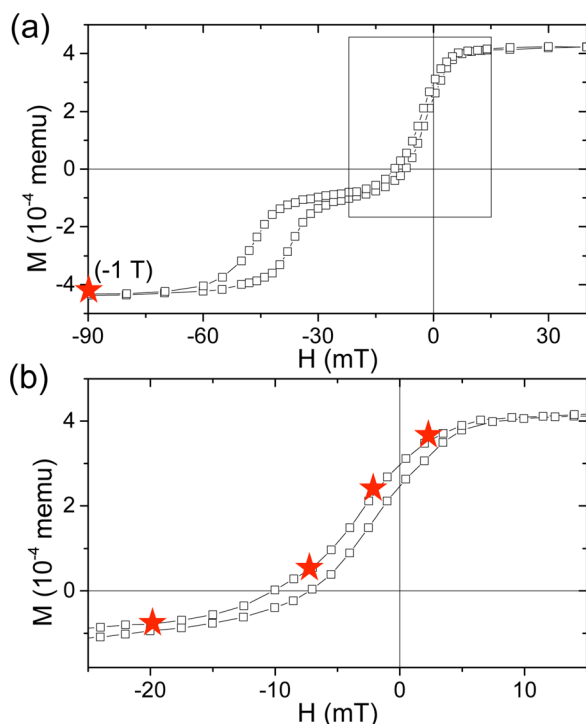


FIG. 2. The entire magnetic hysteresis loop of the multilayer is shown in (a). The boxed area shows the minor loop associated with the free NiFe layer switching and is expanded in (b). Quick tracking PNR scans were made around the minor loop and the red stars represent the applied fields at which full PNR profiles were made.

choose appropriate areas of investigation for the PNR studies. The biased FM NiFe (and CoFe) layers are exchange biased through interactions with the AFM IrMn, clearly seen as a shift in the hysteresis. The reversal of the biased layer can be seen between -60 mT and -30 mT, below which the magnetization of this layer remains pinned. The minor hysteresis loop at low fields (boxed area in Fig. 2(a), and expanded in 2(b)) shows the reversal of the free NiFe layer. It is expected that during these reversal, 90° coupling between the biased and free NiFe layers will manifest.

PNR was performed on the PLATYPUS reflectometer at the OPAL reactor at ANSTO.^{14,15} PNR utilizes the same principles as x-ray reflectometry. Neutrons, however, interact with both the nuclear and spin components of the material under investigation. By selecting the spin polarizations of both the incoming and the detected neutrons using proper polarized neutron optical elements,¹⁵ information about the size and direction of the magnetization within thin layers can be obtained. For non-spin-flip (NSF) PNR, the incoming and detected neutrons have the same polarization (R^{++} or R^{--}), and magnetization that is parallel or antiparallel to the neutron spins and external magnetic field can be observed. Spin-flip (SF) PNR measures incoming and detected neutrons with opposite spin states (R^{+-} or R^{-+}) and is capable of detecting magnetization that is perpendicular to the neutron polarization established by the external field direction. Specular PNR is limited, however, in that it can only measure sample magnetization lying within the film plane and cannot detect magnetization perpendicular to the film. Therefore, together both NSF and SF PNR can be used to obtain the full in-plane magnetization vectors of magnetic layers as a function of depth. Modelling and least squares refinement were performed using the Simulreflec¹⁶ software package.

III. RESULTS AND DISCUSSION

PNR scans at a saturating field of -1 T were first performed in order to obtain a nuclear scattering length density (SLD) profile and saturation magnetization profile of the multilayer. The experimental PNR results and fits at -1 T are shown in Fig. 3(a). As expected, no SF signal was detected, since it is evident from the magnetic hysteresis that at high applied fields all layer magnetizations saturate and align parallel to the field. The nuclear and magnetic SLD profiles used to obtain these values are shown in Fig. 3(b) and the resulting magnetization profile across the multilayer is shown in Fig. 3(c). The nuclear SLDs of both NiFe layers ($9.1 \times 10^{-6} \text{ \AA}^{-2}$) and the CoFe layer ($2.5 \times 10^{-6} \text{ \AA}^{-2}$) correspond to SLDs expected considering the atomic densities and scattering lengths of both materials. The free NiFe layer was observed to have a magnetization of $1.0 \mu_B/\text{f.u.}$ and the biased NiFe magnetization was $0.9 \mu_B/\text{f.u.}$, both of which are roughly equal to the literature bulk value of $0.95 \mu_B/\text{f.u.}$ ¹⁷ The biased CoFe layer magnetization was found to be $2.6 \mu_B/\text{f.u.}$ We identified an interfacial layer between biased NiFe and CoFe. At this interface, the nuclear SLD remained that of NiFe but the magnetization increased; since the nuclear SLD of CoFe is lower than NiFe despite a larger

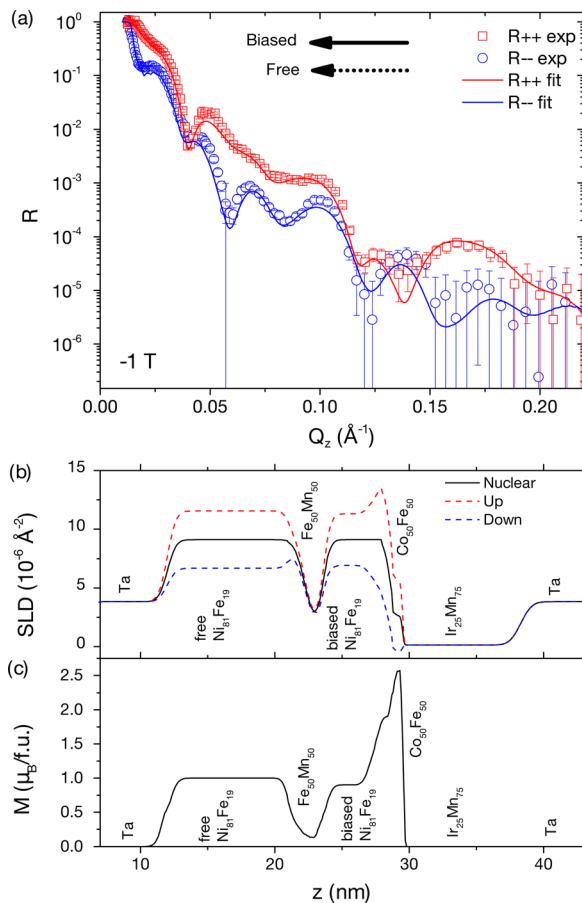


FIG. 3. (a) The non-spin-flip PNR data and fits in the saturated state of the sample. The arrows represent the directions of the biased and free layer magnetizations in the x - y plane of the film. (b) The SLD profile used to fit the data. The solid black line shows the nuclear SLD and the dashed lines show the magnetic SLD. (c) The layer magnetization profile across the sample. In (b) and (c), z is the distance from the underlying SiO_2 layer.

magnetization, the increased interfacial moment likely arises from a small level of CoFe intermixing at the NiFe interface.

In order to get a qualitative understanding of the free NiFe layer behavior, we tracked one NSF channel (R^{--}) and the SF signal (R^{++}) at low scattering vectors, Q_z , around the minor hysteresis loop from a negative (-15 mT) to a positive (5 mT) applied field. For this entire field range, the magnetization of the biased NiFe and CoFe layers is oriented parallel to the positive applied field direction. Both the NSF and SF tracking results are shown in Fig. 4(a), with integrated intensities over a section of the scans in Fig. 4(b). For the R^{--} channel, the overall nature of the curve is retained in the range from -15 mT to -1.5 mT, only deviating at 2.5 mT. This indicates that the projection of the free NiFe magnetization remains aligned in the negative direction until an applied field between -1.5 mT and 2.5 mT. For the R^{++} SF curves, the SF signal increases from -15 mT to -1.5 mT, after which it decreases. This indicates an increase and eventual decrease in the magnetization component perpendicular to the applied field. A simple model of the free NiFe magnetization rotation described by these results is shown in Fig. 4(c), where the free NiFe moment rotates away from the applied field axis, eventually becoming perpendicular with the applied field at around -1.5 mT, where the maximum spin-flip signal was observed. Alternative

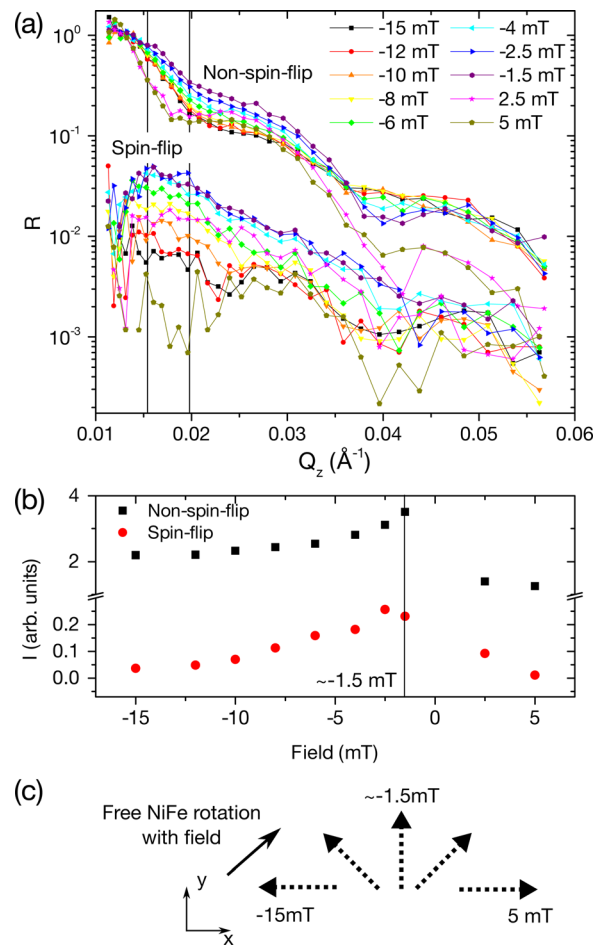


FIG. 4. (a) Tracking scans of the R^{--} non-spin-flip and R^{++} spin-flip channels around the free NiFe hysteresis loop. (b) Integrated intensity for the area between the black vertical lines in (a) from -15 mT to 5 mT. (c) A model of the behavior of the free NiFe magnetization vector (dotted arrow) during reversal. The magnetic field is applied along the x direction.

models of reversal, such as the formation of domains or an out-of-plane spin flip are not viable models, as neither scenario would result in the observation of a strong SF signal.

While tracking the magnetic reversal with the low Q_z PNR signal enabled a qualitative description of the free NiFe magnetization under low fields with respect to the applied field direction, full PNR analysis was performed in order to firmly establish the magnetization vectors of all the magnetic layers as a function of field. The R^{++} , R^{--} , and R^{+-} spin channels were monitored at -20 mT, -8 mT, -2.5 mT, and 2.5 mT (as indicated by the red stars in Fig. 2). For these scans, the nuclear SLD profile obtained from the -1 T scan was fixed during fitting, such that only the magnetization values (magnitude and direction) for the free NiFe, biased NiFe and CoFe, and interfacial layers were free parameters. The data and the fitted models are shown in Fig. 5. The solid and dashed arrows in each plot represent the determined directions of the magnetization in the x - y plane of the sample for the biased and free layers, respectively.

Fig. 5 shows the reflectometry results for small applied fields around the free NiFe layer hysteresis loop. The data at each field were successfully modeled using the saturation magnetization magnitude for each layer (free NiFe: $1\mu_B/\text{f.u.}$,

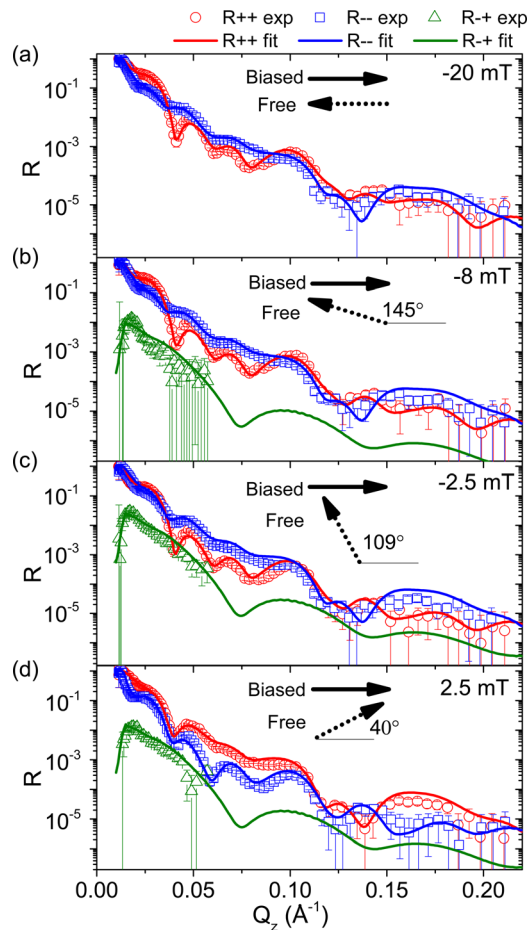


FIG. 5. PNR data and fits taken at -20 mT (a), -8 mT (b), -2.5 mT (c), and 2.5 mT (d). The arrows in each plot represent the magnetization directions of the free and biased layers in plane of the sample.

biased NiFe: $0.9\mu_B/\text{f.u.}$, biased CoFe: $2.6\mu_B/\text{f.u.}$) and only the sizes of the components parallel and perpendicular to the applied field were varied. For the smaller fields, only the low Q_z SF signal (R^-) is displayed, which is due to low counting statistics in the high Q_z region, resulting in large error bars at high Q_z . However, as can be seen in Fig. 5, the primary information needed to fit the SF signal, particularly the intensity that gives the magnitude of the magnetization perpendicular to the field, can be found at low Q_z . The SF signals for each field can be used to measure the magnitude of the magnetization component perpendicular to the applied field. While the SF channel alone cannot uniquely determine the exact magnetization vector of each layer, the perpendicular component can be combined with the component of the magnetization parallel (or antiparallel) to the applied field modeled from the NSF signal in order to ascertain the magnetization size and direction of each layer.

Fig. 5(a) shows the -20 mT PNR curves only for the NSF channels, as no SF signal was observed at this field (see Fig. 4(a)). At -20 mT, the biased NiFe and CoFe layer magnetizations have reversed and are now parallel to the positive field direction and the free NiFe layer has not begun to undergo magnetic reversal so it remains aligned in the negative field direction. Compared with the saturated state detailed above, the magnitude of the free NiFe layer remains

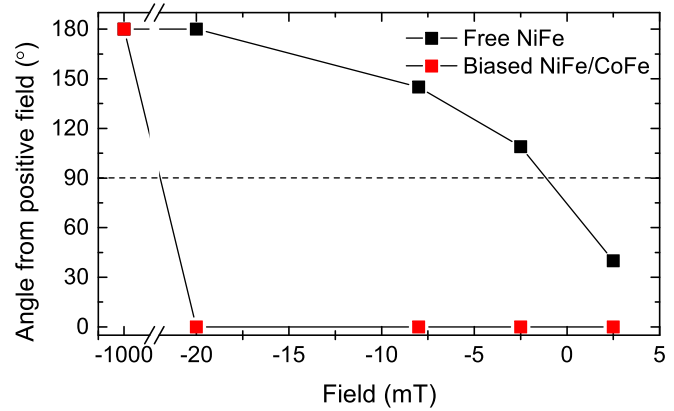


FIG. 6. Angle of the free NiFe and biased NiFe and CoFe layers magnetizations with respect to the positive field direction.

the same and those of the biased NiFe and CoFe layers are slightly reduced, indicating that they have not completely reversed (compare also with Fig. 2(a)). At -8 mT (Fig. 5(b)), the biased layers have fully reversed, remaining aligned in the positive field direction with magnetizations returned to saturation values. The free NiFe magnetization magnitude is equal to the saturation value but has rotated from an antiparallel alignment with the positive field, to an angle of 145° with respect to the positive field and biased layers. This rotation continues at -2.5 mT (Fig. 5(c)), with the free NiFe now at 109° with respect to the biased NiFe and CoFe layers. At 2.5 mT (Fig. 5(d)), the free NiFe magnetization has gone through a direction perpendicular to the applied field and biased layer magnetizations and is orientated at 40° to the positive applied field. The angle of each layer magnetization with respect to the positive field direction is shown in Fig. 6.

These detailed magnetization profiles, along with the tracking scans shown above, demonstrate that during magnetic reversal, there is indeed a 90° orientation of the free and biased FM magnetizations occurring at an applied field of roughly -1.5 mT. Ideally, for device applications, this perpendicular orientation should occur at zero field. Here, however, the free NiFe layer is offset, shifting its hysteresis in the negative field direction. It is then just a question of engineering the system further to reduce the effect of exchange bias on the free NiFe layer (perhaps by adding a thicker or non-magnetic spacer layer between the free and biased FM layers) in order to produce the desired SV with perpendicular coupling at zero magnetic field. An additional solution has been proposed by Liu *et al.*,¹ utilizing a synthetic AFM layer in a completed SV structure.

IV. CONCLUSIONS

In summary, we presented a direct observation of 90° coupling between a free FM layer and a biased FM layer in a NiFe/FeMn/biased NiFe multilayer SV component. Using PNR, we derived magnetization depth profiles under a range of applied magnetic fields as well as qualitatively track the magnetization direction of the free NiFe layer during reversal at low fields. The tracking measurements displayed an increase and subsequent decrease in the spin-flip signal,

signifying that the layer magnetization rotated through an orientation perpendicular to the applied field. Combining this result with more detailed PNR scans at several fields around the free FM layer magnetic hysteresis loop definitively showed that at low fields, the biased NiFe magnetization remained aligned in the applied field direction, and at roughly -1.5 mT, the free NiFe magnetization was oriented at 90° to the biased layer.

ACKNOWLEDGMENTS

This work has been supported by the National Basic Research Program of China (2012CB933102) and National Science Foundation of China (Grant Nos. 11079052 and 11174354).

¹T. Liu, T. Zhu, J. W. Cai, and L. Sun, *J. Appl. Phys.* **109**, 094504 (2011).

²M. Tondra, J. M. Daughton, C. Nordman, D. Wang, and J. Taylor, *J. Appl. Phys.* **87**, 4679 (2000).

³Y. Lu, R. A. Altman, A. Marley, S. A. Rishton, P. L. Trouiloud, G. Xiao, W. J. Gallagher, and S. S. P. Parkin, *Appl. Phys. Lett.* **70**, 2610 (1997).

⁴S. Lacour, H. Jaffrès, F. Nguyen Van Dau, F. Petroff, A. Vaurès, and J. Humbert, *J. Appl. Phys.* **91**, 4655 (2002).

⁵B. Negulescu, D. Lacour, F. Montaigne, A. Gerken, J. Paul, V. Spetter, J. Marien, C. Duret, and M. Hehn, *Appl. Phys. Lett.* **95**, 112502 (2009).

⁶M. E. Filipkowski, J. J. Krebs, G. A. Prinz, and C. J. Gutierrez, *Phys. Rev. Lett.* **75**, 1847 (1995).

⁷P. A. A. van der Heijden, C. H. W. Swüste, W. J. M. de Jonge, J. M. Gaines, J. T. W. M. van Eemeren, and K. M. Schep, *Phys. Rev. Lett.* **82**, 1020 (1999).

⁸J. Camarero, Y. Pennec, J. Vogel, M. Bonfim, S. Pizzini, F. Ernult, F. Fettar, F. Garcia, F. Lançon, L. Billard, B. Dieny, A. Tagliaferri, and N. B. Brookes, *Phys. Rev. Lett.* **91**, 027201 (2003).

⁹S. Matt and B. A. Gurney, *J. Appl. Phys.* **993**, 7229 (2003).

¹⁰Y.-J. Wang, C.-H. Lai, P.-H. Huang, C.-T. Shen, S. Y. Yang, T. S. Chin, H.-H. Lin, T.-M. Hong, H. J. Lin, and C. T. Chen, *Appl. Phys. Lett.* **88**, 112510 (2006).

¹¹Y. F. Liu, J. W. Cai, W. Y. Lai, and G. H. Yu, *J. Appl. Phys.* **103**, 093908 (2008).

¹²G. P. Felcher, R. O. Hilleke, R. K. Crawford, J. Haumann, R. Kleb, and G. Obstrowski, *Rev. Sci. Instrum.* **58**, 609 (1987).

¹³M. R. Fitzsimmons, S. D. Bader, J. A. Borchers, G. P. Felcher, J. K. Furdyna, A. Hoffman, J. B. Kortright, I. K. Schuller, T. C. Schulthess, S. K. Sinha, M. F. Toney, D. Weller, and S. Wolf, *J. Magn. Magn. Mater.* **271**, 103 (2004).

¹⁴M. James, A. Nelson, S. A. Holt, T. Saerbeck, W. A. Hamilton, and F. Klose, *Nucl. Instrum. Methods Phys. Res., Sect. A* **632**, 112 (2011).

¹⁵T. Saerbeck, F. Klose, A. P. LeBrun, J. Fuezi, A. Brule, A. Nelson, S. A. Holt, and M. James, *Rev. Sci. Instrum.* **83**, 081301 (2012).

¹⁶SimulReflec, Lèon Brillouin CEA/CNRS UMR12, Copyright (C) Lab, 2011, free software available at <http://www-llb.cea.fr/prism/programs/simulreflec/simulreflec.html>.

¹⁷D. L. Cortie, K.-W. Lin, C. Shueh, H.-F. Hsu, X. L. Wang, M. James, H. Fritzsche, S. Brück, and F. Klose, *Phys. Rev. B* **86**, 054408 (2012).